Advances in Science and Technology Research Journal

Advances in Science and Technology Research Journal, 2026, 20(3), 74–86
https://doi.org/10.12913/22998624/213533
ISSN 2299-8624, License CC-BY 4.0

Received: 2025.09.30
Accepted: 2025.11.23
Published: 2026.02.01

Experimental tests and analytical model for stick-slip phenomenon reduction with the use of longitudinal tangential vibrations

Mariusz Leus[1*], Marta Rybkiewicz[1], Paweł Gutowski[1]

[1] Faculty of Mechanical Engineering and Mechatronics, West Pomeranian University of Technology in Szczecin, al. Piastów 19, 70-310 Szczecin, Poland
* Corresponding author's email: mariusz.leus@zut.edu.pl

ABSTRACT

The article presents the results of experimental investigations and simulation analyses regarding the potential for partial reduction or complete elimination of the stick-slip phenomenon in sliding motion through the introduction of forced tangential longitudinal vibrations into the contact zone of the friction pair, with precisely defined parameters such as amplitude and frequency. An original analytical model is presented, enabling the selection of optimal parameters of the forced vibrations, under which the stick-slip phenomenon for a given friction pair can be reduced or completely eliminated. The investigations were carried out for three friction pairs comprising C45 steel, GGG40 cast iron, and polytetrafluoroethylene (PTFE), characterized by distinctly different mechanical properties. A very good agreement was obtained between the results of experimental tests and model analyses, demonstrating accurate modeling of frictional phenomena in the contact zone of the friction pair during sliding motion using the adopted computational algorithm.

Keywords: stick-slip phenomenon, vibrations, experimental verification.

INTRODUCTION

Friction-induced stick-slip vibrations constitute a persistent challenge in numerous technological and utility processes, including braking systems [1,2], railway wheel-rail interactions [3,4], motion control in robotic and machine modules [5,6], high-precision machining operations [7,8], and deep-well drilling [9,10]. This phenomenon, characterized by the irregular motion of a sliding body, causes operational instabilities in mechanical systems and accelerates wear of their components [11,12].

The generation of self-excited frictional vibrations results from the variable magnitude of the sliding friction force, which depends on the instantaneous slip velocity. The distinction between the coefficients of static and kinetic friction stems from the elastic-plastic properties of the frictional contact, governed by material characteristics, surfaces texture and contact pressure [13,14]. These coefficients are not constant and exhibit variability. The maximum static friction force increases with the duration of the static phase due to the interlocking of surface asperities and the strengthening of adhesive bonds [15,16]. The kinetic friction force depends on the instantaneous slip velocity and the motion history over the preceding critical interval. Higher values of the kinetic friction coefficient occur during acceleration, while lower values occur during deceleration driving the dynamic instability in frictional systems [17,18].

In industrial applications, stick-slip vibrations constitute a significant challenge in sliding systems with low drive stiffness or operating at low sliding velocities. For each frictional pair, critical values of these parameters can be determined, and exceeding either one effectively prevents the onset of self-excited frictional vibrations [19,20].

An example of a sliding system with low stiffness is the drilling equipment used for deep borehole excavation in the oil mining industry. The high slenderness of these systems, combined with significant frictional forces, predisposes them to friction-induced stick-slip vibrations [9,21–23]. These phenomena increase the costs of drilling operations by accelerating drill bit wear and necessitating reduced penetration rates due to cyclic dynamic stresses, which cause fatigue damage to the structure. The problem is particularly severe in horizontal wells, where the increased sliding contact area between the drilling system and the borehole walls exacerbates frictional resistance [9,10,24,25].

Functioning at low feed rates is typical for machines that require high operational accuracy and perform under high loads, such as machine tools, manipulators, or measuring devices. The occurrence of friction-induced stick-slip vibrations in the operation of sliding guides significantly accelerates the wear of machine components and reduces the positioning accuracy of their moving parts, as the achieved actual position will depend on the amplitude of these vibrations [5–8,26,27].

In some cases, stick-slip vibrations in the operation of machines and devices must be eliminated not only due to disruptions or potential structural damage but also because of the harmful noise generated. While the sound produced by frictional vibrations in stringed musical instruments may be pleasant, the squealing noises from braking and curving are considered a form of environmental noise pollution [1–4,28–30]. A primary example of this type of disruptive noise is the curve squeal generated by stick-slip vibrations during the curving of rail vehicles in large urban areas, where the high frequency of traffic exacerbates their impact [3,4]. This issue also manifests in high-speed rail systems, where high-frequency noise generated by braking mechanisms not only contributes to environmental degradation but also affects passenger ride comfort and the physical and mental health of railway workers [2,29,30]. Moreover, friction-induced stick-slip vibrations pose a serious threat to train safety by causing failures in braking system components, such as brake pad cracking, uneven lining wear, or damage to the caliper mechanism [2,30].

As a result of the widespread occurrence of stick-slip vibrations in mechanical systems and the negative effects of their impact, various methods for their elimination have been developed. During the design phase of a sliding system, it is essential to select materials with low friction coefficients for the contact surfaces [31,32], achieve optimal surface roughness [31,32], including intentional micro texturing [27,33], and choose a lubrication method appropriate for the system's intended operating conditions [34,35]. Avoiding self-excited frictional vibrations is also possible by ensuring high drive system stiffness [19,36], minimizing surface pressures [32], and determining safe feed rate ranges through the identification of friction parameters [7].

A promising method for eliminating stick-slip friction vibrations is so called dynamic lubrication, which involves introducing external mechanical vibrations with selected parameters into the sliding contact area [10,28,37,38]. This method is an alternative to traditional lubrication techniques, particularly under challenging conditions such as elevated temperatures, high humidity, or contamination, where conventional lubricants tend to degrade and become ineffective. This method facilitates dynamic adaptation to varying operating conditions through the selection of forced vibration parameters. Moreover, it remains effective under high loads and is relatively straightforward to implement, even in existing systems.

Forced vibrations with low to medium frequencies, up to 500 Hz, are increasingly utilized in the drilling process for the oil mining industry [22,23], particularly in horizontal drilling, where elevated frictional resistances occur [9,10]. This technology is distinguished by its environmental friendliness, as it does not generate pollutants. Additionally, initial attempts are being made to employ high-frequency vibrations, including ultrasonic ones, to eliminate brake [1,28] and curve squeal [3].

The application of dynamic lubrication to reduce frictional forces in sliding motion has been extensively studied both theoretically and experimentally, as reflected in numerous works on tribology and contact mechanics [33,39–43]. However, the suppression of stick-slip frictional vibrations, despite their significant impact on the stability of motion in mechanical systems, is often addressed peripherally, with few studies focusing solely on this phenomenon. The earliest mentions of the potential use of forced vibrations to suppress stick-slip appeared in the 1950s and 1960s in the pioneering works of Bowden and Tabor [44], Tolstoi [45,46], Lenkiewicz [47], and Rabinowicz [17], which laid the theoretical and

experimental foundations for further research into the mechanisms and control of stick-slip.

Subsequent theoretical and experimental studies have demonstrated that the effective elimination of the stick-slip phenomenon through dynamic lubrication requires appropriate selection of materials for the contacting surfaces as well as the optimization of forced vibrations parameters such as their direction and velocity amplitude [38,48]. Most research focuses on normal vibrations, perpendicular to the contact plane. For instance, Abdo et al. [49,50], Abdo, and Zaier [51], as well as Kröger et al. [32], employ external mechanical vibrations generated by actuators, whereas Neubauer et al. [52], Popp and Rudolph [53,54] and Wang [55] utilize a variable normal force pressing the contact surfaces. Although tangential vibrations have received comparatively less attention, notable studies in this area have been presented by Popov et al. [56], Teidelt et al. [57], and by the authors of the present work [40]. Recent studies by Luo [58,59] investigate the effectiveness of tangential vibrations in the ultrasonic range for eliminating stick-slip under various contact conditions, such as dry [58], oil-lubricated [58], or solid-lubricated contacts [59]. It has been shown that for dry and solid-lubricated contacts, the effects are predictable, whereas in oil-lubricated contacts, additional tangential vibrations can exacerbate frictional vibration.

The paper presents the results of experimental studies on the effective reduction and complete elimination of the stick-slip phenomenon in sliding motion by introducing forced tangential vibrations with precisely defined parameters, such as amplitude and frequency, into the contact area of the friction pair. An original analytical model is presented, enabling the simulation analysis of the stick-slip phenomenon in sliding motion. The model facilitates the optimal selection of forced vibration parameters, at which the stick-slip phenomenon can be mitigating or completely eliminated for a given friction pair. The verification and validation of the model were conducted for three friction pairs composed of such materials as steel, cast iron, and Teflon, which exhibit fundamentally different mechanical properties. A very good agreement was obtained between the results of experimental studies and model analyses, confirming the accuracy of the adopted computational algorithm in modeling the friction phenomena occurring within the contact zone of the friction pair during sliding motion.

EXPERIMENTAL INVESTIGATIONS

Experimental investigations were conducted using a test stand described in detail in the literature [48]. A view of the mechanical part of the experimental stand, together with a block diagram of the measurement and data processing system, is presented in Figure 1.

The core component of the test stand is a sliding pair comprising the upper specimen *A* and the lower specimen *B*. During the experiments, the upper specimen is displaced relative to the lower specimen at a prescribed velocity v_d by means of the drive system. The lower specimen can be introduced to oscillate at any moment in the direction parallel to the displacement axis of the upper specimen by means of a piezoelectric vibration exciter. The drive stiffness k_d is adjusted using mechanism *E*, which incorporates a spring of specified stiffness.

The measurement system integrated into the test stand facilitates continuous monitoring of the drive force F_d, the acceleration of the upper specimen $\ddot{x}$ and the lower specimen $\ddot{u}$, the displacement of the upper specimen x, and the drive system displacement s_d. The drive force is measured with a ring-type force sensor *D* with TF-3/120 strain gauges operating in a full-bridge configuration. This force sensor was calibrated for a load range of 0–50 N, with a measurement error determined during calibration to be ≤ 2% of the measured value. The accelerations are measured using miniature ICP-type M352C65 acceleration sensors *H* from PCB, with a measurement range of ±50 g, an accuracy error of ±1% at frequencies of 100–1999 Hz, and ±2.5% at frequencies of 2–10 kHz. The displacements of the sliding body x and of the drive system s_d are measured using WA/50 inductive displacement transducers *G* from HBM, aligned parallel to the axis of motion, with a measurement range of 0–50 mm and a linearity deviation of ≤ ±0.2%.

The experimental investigations were conducted in two stages. First, the influence of the material type of the mating sliding pair on the possibility of stick-slip motion occurrence was examined. The measurements were performed for three friction pairs: C45 steel – C45 steel, C45 steel – GGG40 cast iron, and C45 steel – polytetrafluoroethylene PTFE, for two values of normal pressure $p_n = 0.063$ N/mm^2 and $p_n = 0.104$ N/mm^2, at a drive velocity of $v_d = 0.5$ mm/s and a drive stiffness of $k_d = 11.7$ N/mm. Experimental tests

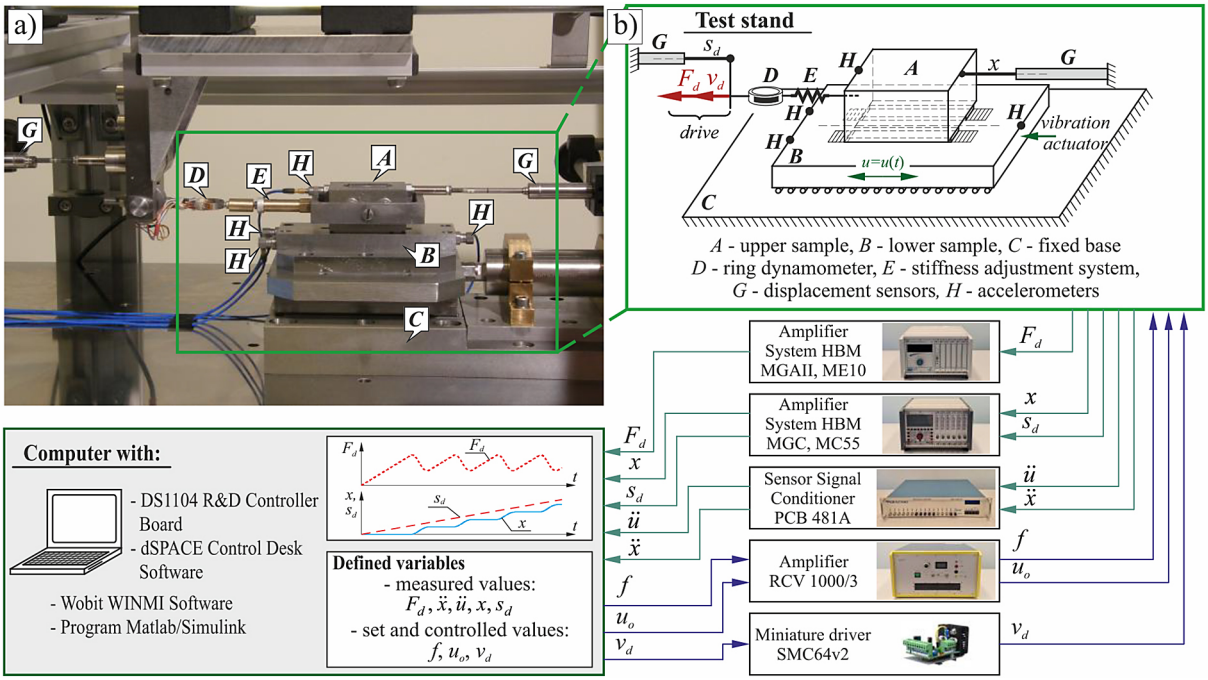

Figure 1. Test stand: a) photograph of the mechanical part prepared for test, b) block diagram of the measurement and data handling system

were carried out under normal room conditions, at temperatures ranging from 22 °C to 26 °C and humidity ranging from 48% to 60%. It was assumed that the effect of temperature and humidity variations within the specified range on measurement accuracy is negligible.

The values of the R_a parameter of the contacting surfaces of the tested sliding pairs, as well as the values of the tangential contact stiffness coefficient k_t for these pairs at the specified normal pressures p_n are presented in Table 1. The k_t values for the selected friction pairs were determined experimentally in accordance with the procedures described in [43].

In the experiments, change in the driving force F_d, the displacement of the upper specimen x, and the drive displacement s_d were recorded. Figure 2 presents a photograph of the sliding pairs prepared for experimental testing, along with representative time courses of the measured quantities (F_d, x and s_d) at a normal pressure of p_n = 0.063 N/mm^2 , when the motion of the upper specimen occurred solely with the lower specimen immobilized, i.e. without induced vibrations of the lower specimen. For the C45 steel – polytetrafluoroethylene (PTFE) sliding pair, which exhibited the lowest contact stiffness, no stick-slip behavior was observed at any applied normal pressure. For the other two sliding pairs, stick-slip motion occurred at all tested values of p_n.

In the second stage, for the sliding pairs exhibiting stick-slip motion, experimental investigations were performed to assess the potential for partial or complete reduction of this phenomenon by introducing into the contact zone forced tangential longitudinal vibrations with precisely defined parameters, such as frequency f and amplitude u_0. The experiments were performed with harmonic excitation of the lower specimen at a prescribed vibration velocity $\dot{u} = v_a \cdot \cos(\omega t)$, where $v_a = u_o \cdot \omega$ is the amplitude of the vibration velocity and $\omega = 2\pi f$ is the angular frequency of the vibrations. The parameters defined during the measurements required to calculate v_a, were the frequency f and the amplitude u_o of forced vibrations.

At this stage of the research, in the first phase of motion, for t = 0 – 8 s, the displacement of the upper specimen was carried out with the lower specimen fixed, whereas in the second phase, for t = 8 – 16 s under forced tangential longitudinal vibrations of the lower specimen. The experiments were carried out for five different frequencies f specifically 1, 2, 3, 4, and 5 kHz, with a constant vibration amplitude of u_o = 0.02 μm. For these adopted values of f and u_o, the vibration velocity amplitude v_a was 0.126, 0.251, 0.377, 0.503 and 0.628 mm/s respectively.

In Figures 3 and 4, exemplary waveforms are presented for steel-steel pair under both adopted

Table 1. Dependence of the tangential contact stiffness coefficient k_t for the selected sliding pairs on the normal pressure

Sliding pair	R_a lower specimen/upper specimen [μm/μm]	k_t [N/μm]	
		p_n = 0.063 [N/mm²]	p_n = 0.104 [N/mm²]
C45-C45	0.44/1.35	77.52	95.66
C45-GGG40	0.44/1.14	71.15	107.74
C45-PTFE	0.44/2.05	4.89	6.42

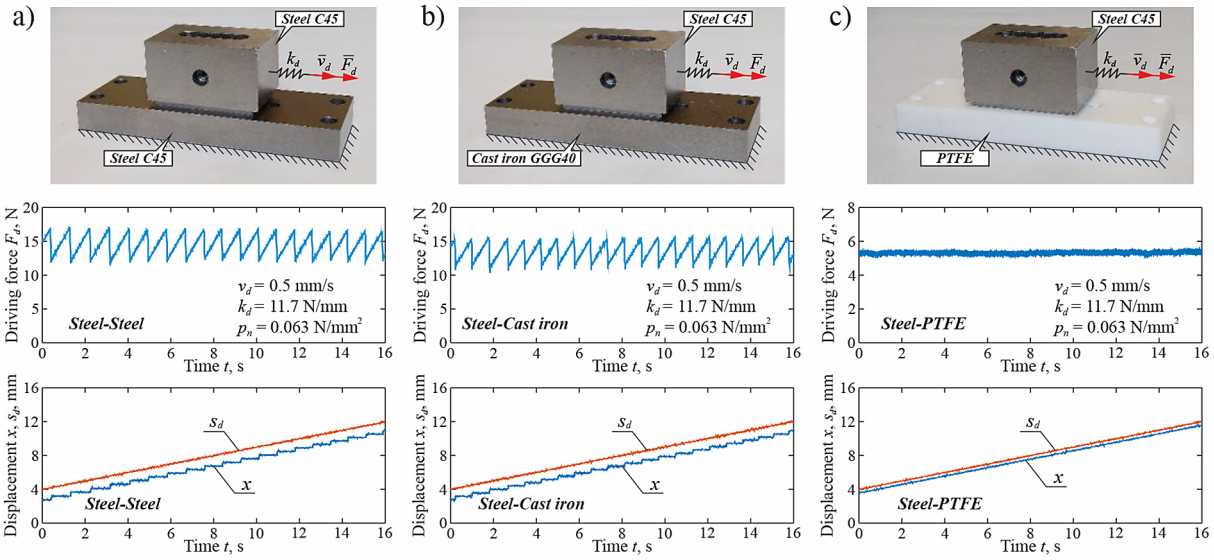

Figure 2. Photographs of specimens prepared for testing and time courses of the driving force F_d, displacements x and s_d, for tested pairs: a) steel-steel, b) steel-cast iron, c) steel-PTFE

values of normal pressure, within the time interval t = 8–12 s, i.e., immediately after the introduction of tangential vibrations into the contact zone. In the first panels of these plots, the corresponding responses without vibrations have also been added, which makes it easier to evaluate the influence of the vibration velocity amplitude on stick-slip phenomenon.

The presented plots indicate that with increasing frequency f of the forced vibrations of the base and consequently with increasing vibration velocity amplitude v_a, the stick-slip motion gradually diminished – the difference between the maximum and minimum values of the driving force F_d decreases, and the duration of adhesion between the upper and lower specimens shortens.

The presented waveforms also show that further increasing the vibration frequency (up to 5 kHz) resulted in a reduction of the driving force required to maintain sliding motion in both cases. This effect was expected, as according to the results of model analyses and experimental tests [40,60], the introduction of longitudinal tangential vibrations with a vibration velocity amplitude v_a greater than the driving velocity v_d into the contact zone between the sliding body and the base leads to a reduction in the friction force in the contact surfaces.

ANALYTICAL MODEL AND ITS EXPERIMENTAL VERIFICATION

The development of analytical and numerical models to analyze the effectiveness of dynamic lubrication in the stick-slip phenomenon reduction or its elimination in real sliding systems is essential for enhancing the practical utility of this method and enabling real-time control of such systems.

Accurate modeling of sliding motion dynamics, incorporating the properties of contact interfaces, the drive system, and externally induced vibrations, ensures a strong correlation between numerical and experimental results. This establishes a robust foundation for comprehensive numerical

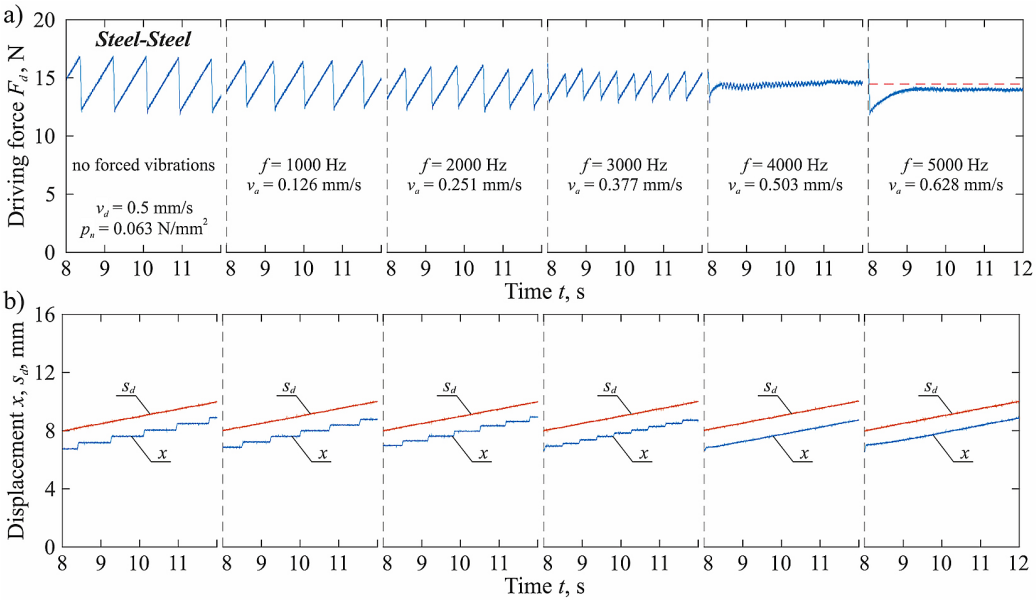

Figure 3. Reduction of stick-slip with increasing frequencies of forced tangential vibrations for a steel-steel contact at constant normal pressure p_n = 0.063 N/mm²: a) driving force F_d, b) displacements of the sliding body x and drive s_d; v_d = 0.5 mm/s, u_0 = 0.02 µm

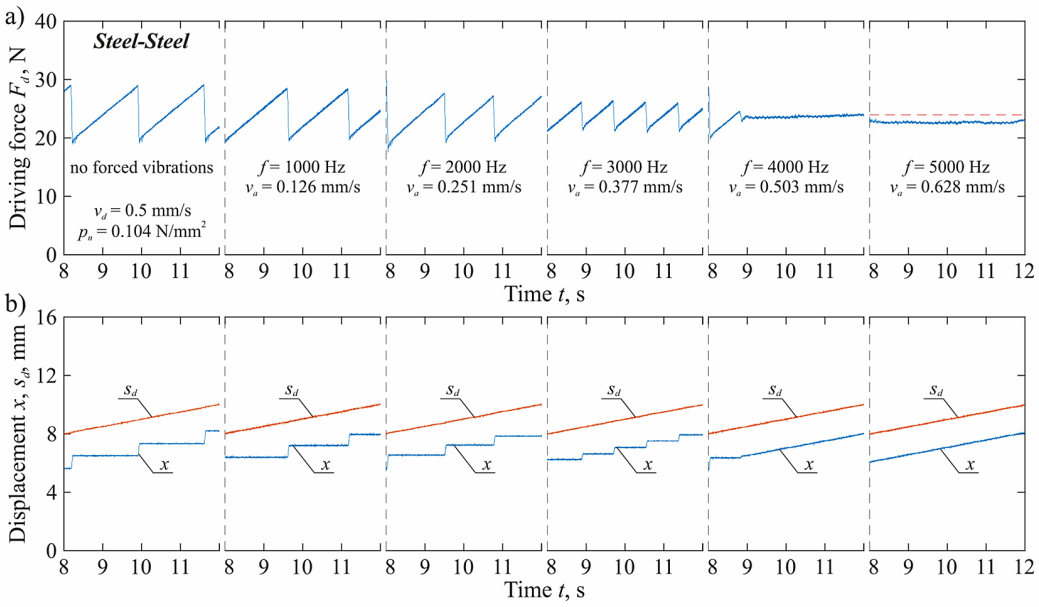

Figure 4. Reduction of stick-slip with increasing frequencies of forced tangential vibrations for a steel-steel contact at constant normal pressure p_n = 0.104 N/mm²: a) driving force F_d, b) displacements of the sliding body x and drive s_d; v_d = 0.5 mm/s, u_o = 0.02 µm

analyses across a wide range of system parameters. The methodology for modeling the contact zone of a friction pair and the fundamental mathematical relationships employed in the developed numerical model for analyzing the stick-slip phenomenon in sliding motion, as well as its partial reduction or complete elimination through longitudinal tangential vibrations, are presented in the form of a block diagram in Figure 5.

In part (a) of this figure, the model used for calculation, consisting of an upper body shifted over an oscillating base, along with the method for modeling the contact zone, is shown. In part (b) od this figure, the developed computational algorithm for determining the driving force F_d, the friction force F_f, as well as the displacement x, velocity $\dot{x}$ and acceleration $\ddot{x}$ of the shifted body is presented.

The dynamic properties of the drive system are modeled using a spring-damper element with stiffness k_d and damping h_d. The friction force is calculated using the dynamic LuGre model [13], which describes it as a function of the elastic deformation s in the contact zone, the rate $\dot{s}$ of change of this deformation, and the relative velocity v_r between the contacting bodies. This approach facilitates effective modeling of the behavior of real contact areas under constant surface pressure and a varying tangential force.

The actual contact is established through the interlocking of surface roughness asperities, which are randomly arranged. Dynamic friction models, such as the LuGre model, represent these random asperity interactions using bristle spring-damping elements (Figure 5a). The LuGre model's selection for numerical analysis of stick-slip vibrations and their modulation by forced vibrations was presented in the authors' previous work [37]. Consequently, the frictional contact properties are described by coefficients k_t and h_t, representing tangential stiffness and damping, respectively. These coefficients are determined empirically and are dependent on multiple factors, including contact temperature, the kind of materials, roughness of the interacting surfaces and the magnitude of normal pressures.

The methodology enables modeling of pre-sliding displacement, which involves micro-scale motion occurring before the onset of macroscopic sliding. The resistance due to this initial micro-displacement corresponds to the static friction. To model stick-slip phenomenon, the function $g(v_r)$, which defines the friction force in steady-state conditions, must account for the Stribeck effect. This effect is characterized by a rapid decrease in friction force during the transition from rest to macroscopic sliding motion, which is the primary cause of friction-induced vibrations.

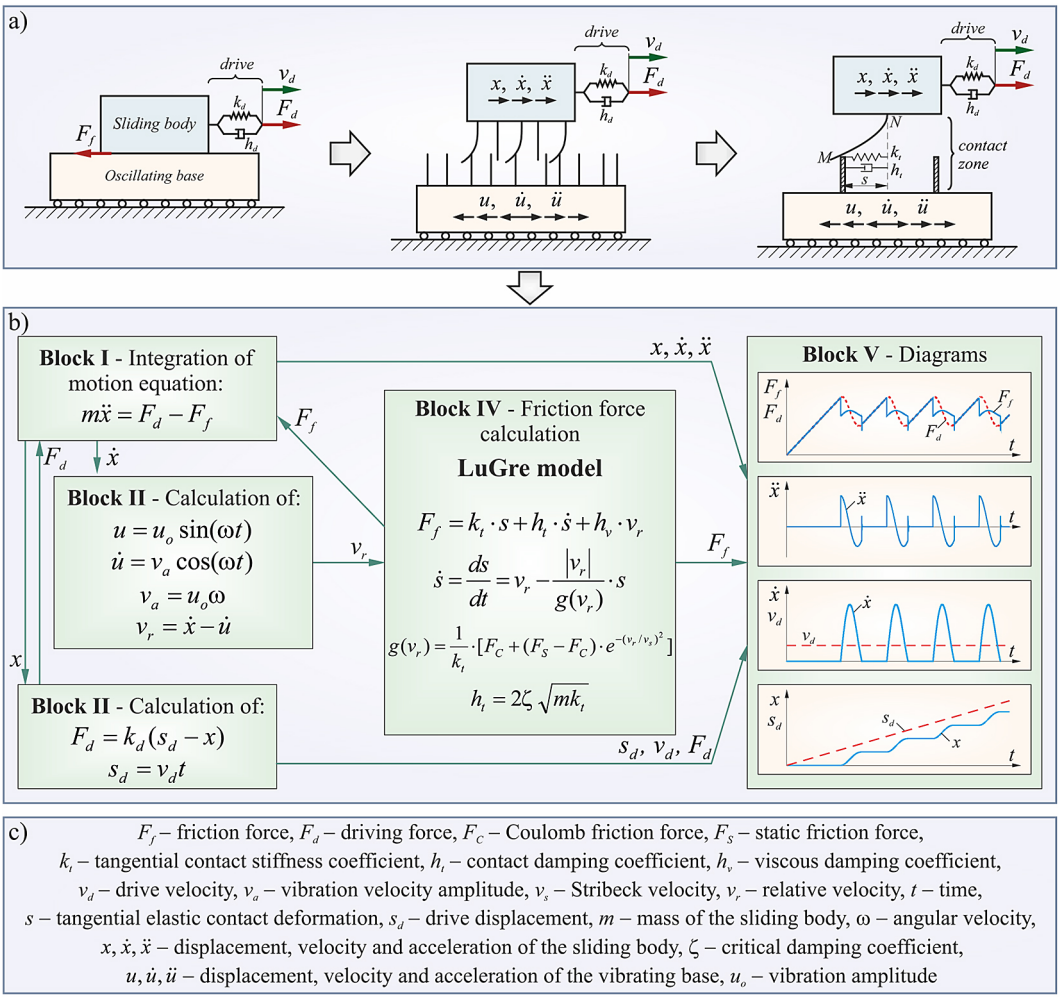

Figure 5. Block diagram of the analytical model: a) friction pair, modelling contact zone and drive, b) algorithm for computing drive F_d and friction F_f forces with the dynamic LuGre model, c) notation

Incorporating the rate of change of elastic bristle deformations in the $h_t \cdot \dot{s}$ term of the friction force equation captures the frictional lag phenomenon, distinguished by hysteresis in the friction force during velocity increase and decrease. The $h_v \cdot v_r$ term in this equation describes the viscous component of the friction force, which increases with the relative sliding velocity and is particularly significant for lubricated contacts.

The numerical model implemented in Matlab Simulink was calibrated to the real sliding system of the experimental test rig. Numerical studies were performed with the drive velocity v_d, normal pressures p_n, and tangential contact stiffness k_t consistent with those used in the experimental tests. Based on the measured value of the contact stiffness (Table 1), the h_t contact damping coefficient in the tangential direction was determined, assuming a critical damping coefficient of $\zeta = 1$ [15]. Given that all investigated contacts are dry connections, the viscous damping coefficient h_v was set to zero. Based on the friction characteristics derived from preliminary experiments on the measurement set up, the friction coefficient μ and maximum static friction force F_s were determined. The value of the Stribeck velocity v_S was adopted based on data from the literature [15]. The values of the parameters for the LuGre friction model incorporated into the numerical model are compiled in Table 2.

Sample comparisons of experimentally measured and numerically determined time courses of F_d, x, and s_d under a contact pressure p_n = 0.063 N/mm^2 and forced vibration frequencies of f = 1000 Hz and f = 3000 Hz for steel-steel and steel-cast iron contact interfaces are presented in Figures 6 and 7. Excellent agreement was achieved for both the time courses of the drive force F_d and the

Table 2. Simulation parameters and value in the LuGre model

Parameters	Symbols	Value				Unit
		C45-C45 p_n = 0.063 [N/mm^2]	C45-C45 p_n = 0.104 [N/mm^2]	C45-GGG40 p_n = 0.063 [N/mm^2]	C45-GGG40 p_n = 0.104 [N/mm^2]	
Mass of upper specimen	m	1.5	1.5	1.5	1.5	[kg]
Friction coefficient	μ	0.193	0.193	0.176	0.176	[–]
Drive stiffness coefficient	k_d	11.7	11.7	11.7	11.7	[N/mm]
Drive damping coefficient	h_d	0	0	0	0	[Ns/m]
Drive velocity	v_d	0.5	0.5	0.5	0.5	[mm/s]
Contact stiffness coefficient	k_t	77.52	95.66	71.15	107.74	[N/m]
Contact damping coefficient	h_t	2.15×10^4	2.39×10^4	2.07×10^4	2.54×10^4	[Ns/m]
Viscous damping coefficient	h_v	0	0	0	0	[Ns/m]
Coulomb friction force	F_c	14.49	23.94	13.23	21.86	[N]
Static friction force	F_s	17.38	29.92	15.88	26.67	[N]
Stribeck velocity	v_s	0.0005	0.0005	0.0005	0.0005	[m/s]

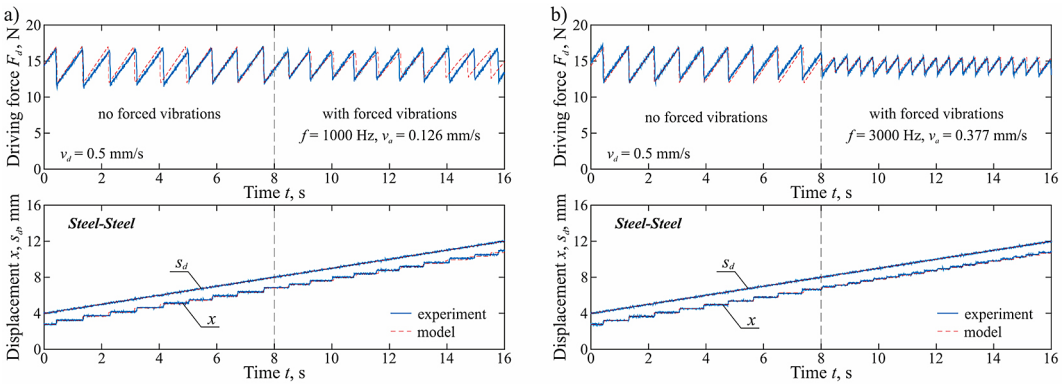

Figure 6. Comparison of experimental and simulated time courses of drive force F_d and displacements x and s_d, for the steel-steel pair: a) f = 1000 Hz, v_a = 0.126 mm/s, b) f = 3000 Hz, v_a = 0.377 mm/s; p_n = 0.063 N/mm^2, v_d = 0.5 mm/s, u_o = 0.02 µm

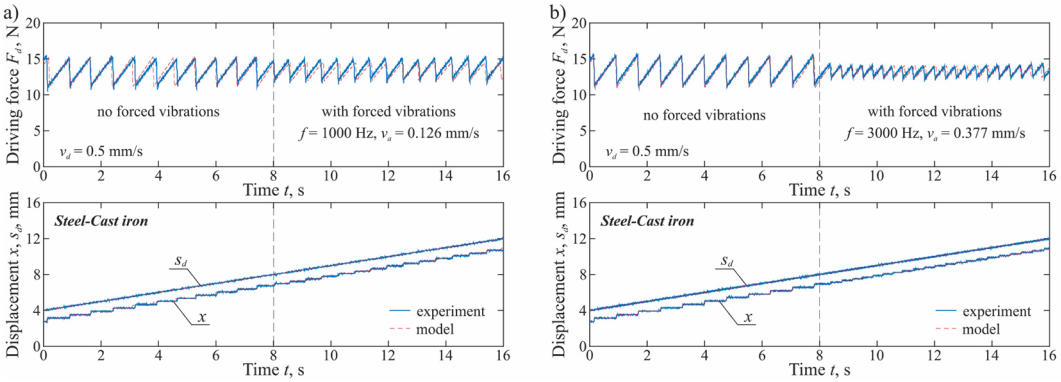

Figure 7. Comparison of experimental and simulated time courses of drive force F_d and displacements x and s_d, for the steel-cast iron pair: a) f = 1000 Hz, v_a = 0.126 mm/s, b) f = 3000 Hz, v_a = 0.377 mm/s; p_n = 0.063 N/mm^2, v_d = 0.5 mm/s, u_o = 0.02 μm

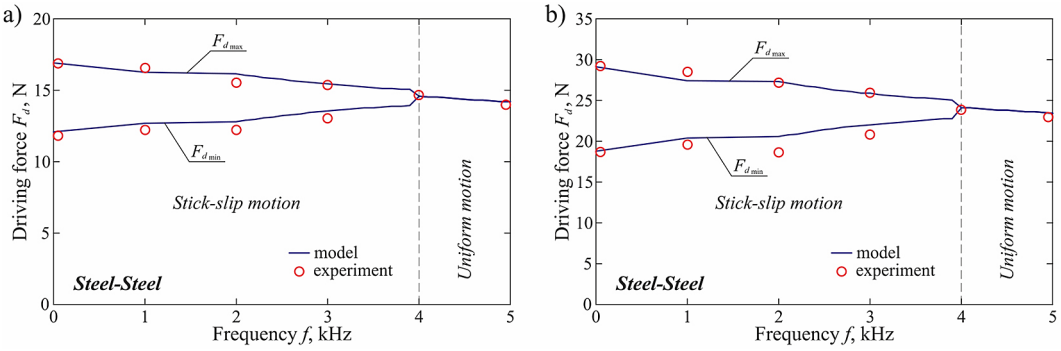

Figure 8. The variation of the maximum F_{dmax} and minimum F_{dmin} driving forces as a function of frequency, determined experimentally and numerically for the steel–steel pair: a) p_n = 0.063 N/mm^2, b) p_n = 0.104 N/mm^2

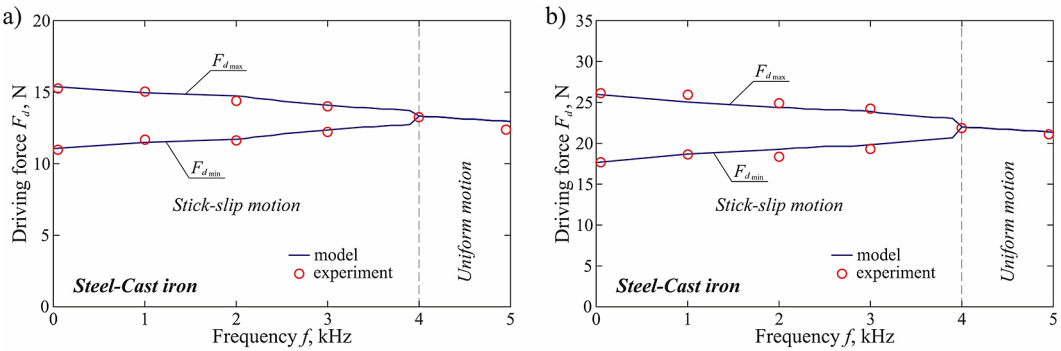

Figure 9. The variation of the maximum F_{dmax} and minimum F_{dmin} driving forces as a function of frequency, determined experimentally and numerically for the steel-cast iron pair: a) p_n = 0.063 N/mm^2, b) p_n = 0.104 N/mm^2

stepwise displacement x of the sliding specimen. These results confirm that the model accurately captures stick-slip vibrations and associated frictional behavior, while effectively predicting the influence of forced longitudinal tangential vibrations on the reduction of stick-slip displacement amplitude.

From a series of plots, such as those shown in Figures 6 and 7, determined for various frequencies of forced vibrations f and illustrating the temporal variations of the drive force F_d over time t, the maximum and minimum drive force values were extracted for successive stick-slip vibration periods within the time interval t = 8–16. Based

on the calculated average values for the maximum and minimum magnitudes of this force, composite plots were generated to illustrate the dependence of variations in the driving force F_d as a function of frequency f.

Figure 8 illustrates these dependencies for steel-steel interface under both assumed normal pressure values, whereas Figure 9 presents the corresponding results for the steel-cast iron interface. The presented plots indicate that for the investigated sliding pairs, as the frequency of forced vibration increases, the amplitude of the driving force variations gradually diminishes, reaching complete suppression at frequency of f = 4 kHz, where the vibration velocity amplitude v_a equals to the driving velocity v_d. Simulation tests also indicate the phenomenon of decreasing the drive force required to maintain sliding motion with further increasing frequency of forced vibrations, as demonstrated in the presented plots during the phase of uniform motion.

CONCLUSIONS

The conducted experimental investigations and simulation analysis have demonstrated that the influence of forced longitudinal tangential vibrations of the base, along which sliding motion is realized, on the stick-slip phenomenon is highly complex. These vibrations can lead to a reduction or even a complete elimination of this phenomenon. The degree of this reduction depends on the amplitude of the vibration velocity v_a relative to the drive velocity v_d. In the range where $v_a < v_d$ only partial reduction of the stick-slip motion occurs. The intensity of this reduction increases with the rise in the value of v_a, which, in the presented studies, resulted from an increase in the frequency f of the forced vibrations while maintaining a constant amplitude u_o. Complete elimination occurs when the amplitude of the vibration velocity is at least equal to or greater than the drive velocity.

The excellent agreement between the results of experimental tests and numerical calculations indicates that the developed analytical model and numerical computational procedures enable not only an accurate reproduction of the stick-slip phenomenon of the sliding motion of the tested friction pairs but also the phenomenon of its partial reduction or complete elimination under the influence of high-frequency forced longitudinal tangential vibrations introduced into the contact area. Therefore, the developed model can be successfully employed for simulation tests of the risk of stick-slip motion occurring in a dynamic systems and for numerical analyses to determine the conditions that the system must meet to avoid such motion.

However, it must be noted that the developed model requires more extensive verification and validation with different friction pair materials, varying surface pressures, and different microgeometries of the contacting surfaces of the friction pairs.

REFERENCES

1. Zhao X., Gräbner N., von Wagner U. Avoiding creep groan: Investigation on active suppression of stick-slip limit cycle vibrations in an automotive disk brake via piezoceramic actuators. Journal of Sound and Vibration. 2019; 441: 174–186. https://doi.org/10.1016/j.jsv.2018.10.049
2. Xie S., Liu G., Xiang Z., Liu Z., Xiao Z., Tang B., et al. Friction-induced stick–slip vibration control via composite design of surface macro-grooves and micro-textures. Tribology Letters. 2025; 73(1): 28. https://doi.org/10.1007/s11249-025-01964-7
3. Kropp W., Theyssen J., Pieringer A. The application of dither to mitigate curve squeal. Journal of Sound and Vibration. 2021; 514(116433): 1–17. https://doi.org/10.1016/j.jsv.2021.116433
4. Thompson D.J., Squicciarini G., Ding B., Baeza L. A state-of-the-art review of curve squeal noise: phenomena, mechanisms, modelling and mitigation. Noise and Vibration Mitigation for Rail Transportation Systems, 139, Berlin, Heidelberg: Springer; 2018. https://doi.org/10.1007/987-3-319-73411-8_1
5. Chuang Y.J., Chang H., Sun Y.T., Tsung T.T. Stick–slip in hand guidance of palletizing robot as collaborative robot. International Journal of Advanced Robotic Systems. 2022; 19(5): 1–8. http://doi.org/10.1177/17298806221131138
6. Owen W.S., Croft E.A. The reduction of stick-slip friction in hydraulic actuators. IEEE/ASME Transactions on Mechatronics. 2003; 8(3): 362–371. http://doi.org/10.1109/TMECH.2003.816804
7. Yang J., Zhou H., Li S., Chen J., Xiang H. Analysis of the critical Stick–slip velocity of CNC machine tool combining friction parameters identification and dynamic model. International Journal of Advanced Manufacturing Technology. 2024; 131: 1849–1865. https://doi.org/10.1007/s00170-024-13202-w
8. Iklodi Z., Piiroinen P.T., Franco O., Beudaert X., Dombovari Z. Stick–slip oscillations in the low feed linear motion of a grinding machine due to dry friction and backlash. International Journal of

Non-Linear Mechanics. 2025; 168: 1–12. http://doi.org/10.1016/j.ijnonlinmec.2024.104940

9. Zhu X., Tang L., Yang Q. A literature review of approaches for stick-slip vibration suppression in oilwell drillstring. Advances in Mechanical Engineering. 2014; 2014: 1–17. http://doi.org/10.1155/2014/967952
10. Tang L., Zhang S., Zhang X., Ma L., Pu B. A review of axial vibration tool development and application for friction-reduction in extended reach wells. Journal of Petroleum Science and Engineering. 2021; 199(108348): 1–12. http://doi.org/10.1016/j.petrol.2021.108348
11. Mfoumou G.S., Kenmoé G.D., Kofané T.C. Computational algorithms of time series for stick-slip dynamics and time-delayed feedback control of chaos for a class of discontinuous friction systems. Mechanical Systems and Signal Processing. 2019; 119: 399–419. http://doi.org/10.1016/j.ymssp.2018.09.034
12. Maegawa S., Itoigawa F. Design method for suppressing stick-slip using dynamic vibration absorber. Tribology International. 2019; 140(105866): 2–8. http://doi.org/10.1016/j.ymssp.2018.09.034
13. Canudas de Wit C., Lischinsky P., Åström K.J., Olsson H. A new model for control of systems with friction. IEEE Transactions on Automatic Control. 1995; 40(3): 419–425. https://doi.org/10.1109/9.376053
14. Zhang Q.X., Mo J.L., Xiang Z.Y., Liu Q.A., Tang B., Jin W.W., et al. The influence of interfacial wear characteristics on stick-slip vibration. Tribology International. 2023; 185(108535): 1–14. https://doi.org/10.1016/j.triboint.2023.108535
15. Olsson H. Control Systems with Friction. Doctoral Thesis (monograph). Lund University, 1996.
16. Ozaki S., Hashiguchi K. Numerical analysis of stick-slip instability by a rate-dependent elastoplastic formulation for friction. Tribology International. 2010; 43(11): 2120–2133. http://doi.org/10.1016/j.triboint.2010.06.007
17. Rabinowicz E. The intrinsic variables affecting the stick-slip process. Proceedings of the Physical Society of London. 1958; 71: 668–675. http://doi.org/10.1088/0370-1328/71/4/316
18. Olsson H., Astrom K.J., Canudas de Wit C., Gäfvert M., Lischinsky P. Friction Models and Friction Compensation. European Journal of Control. 1998; 4: 176–195. http://doi.org/10.1016/S0947-3580(98)70113-X
19. Oprişan C.M., Chiriac B., Carlescu V., Olaru D.N. Influence of the stiffness and the speed on the stick-slip process. IOP Conference Series: Materials Science and Engineering, 997, IOP Publishing Ltd; 2020. http://doi.org/10.1088/1757-899X/997/1/012016
20. Armstrong-Hélouvry B., Dupont P., Canudas de Wit C. A Surtvey of models, analysis tools and compensation methods for the control of machines with friction. Automatica. 1994; 30(7): 1083–1138. http://doi.org/10.1016/0005-1098(94)90209-7
21. Aarsnes U.J.F., Di Meglio F., Shor R.J. Avoiding stick slip vibrations in drilling through startup trajectory design. Journal of Process Control. 2018; 70: 24–35. http://doi.org/10.1016/j.jprocont.2018.07.019
22. Abdo J., Al-Anqoudi I., Al-Sharji H. Experimental evaluations for the effects of amplitude and frequency of vibration on the friction of coiled tubing in hydrocarbon drilling operations. ASME 2014 International Design Engineering Technical Conferences & Computers and Information in Engineering Conference, New York: 2014. http://doi.org/10.1115/DETC2014-34124
23. Wahyudi A., Biyanni H., Tamuli A., Agarwal C., Hermawirawan L., Nowfal M., et al. First Trial of On-Demand Activated Axial Agitation System on Abu Dhabi Offshore Operation. International Petroleum Technology Conference, Dhahran, Saudi Arabia: 2024.
24. Liu W., Ni H., Wang Y., Guo Y., Gao Y., He P. Dynamic modeling and load transfer prediction of drillstring axial vibration in horizontal well drilling. Tribology International. 2023; 177(107986). http://doi.org/10.1016/j.triboint.2022.107986
25. Yang L., Sitong C., Shuyong W., Haijun T., Xingyun X., Tianshou M. The influence of surface rocking motion on the dynamic responses of drillstring during horizontal well drilling. Results in Engineering. 2025: 106757. http://doi.org/10.1016/j.rineng.2025.106757
26. Liu W., Zhang S., Lin J., Xia Y., Wang J., Sun Y. Advancements in accuracy decline mechanisms and accuracy retention approaches of CNC machine tools: a review. International Journal of Advanced Manufacturing Technology. 2022; 121: 7087–7115. https://doi.org/10.1007/s00170-022-09720-0
27. Fu Y., Yang J., Wang H., He Y. Effect of laser-textured micro dimples on inhibition of stick-slip phenomenon of sliding guideway. Industrial Lubrication and Tribology. 2022; 74(1): 34–44. http://doi.org/10.1108/ILT-08-2021-0339
28. Balaram B., Santhosh B., Awrejcewicz J. Frequency entrainment and suppression of stick–slip vibrations in a 3 DoF discontinuous disc brake model. Journal of Sound and Vibration. 2022; 538(117224): 1–17. http://doi.org/10.1016/j.jsv.2022.117224
29. Xiang Z.Y., Chen W., Mo J.L., Liu Q.A., Fan Z.Y., Zhou Z.R. The effects of the friction block shape on the tribological and dynamical behaviours of high-speed train brakes. International Journal of Mechanical Sciences. 2021; 194(106184). http://doi.org/10.1016/j.ijmecsci.2020.106184
30. Wang Q., Wang Z., Mo J., Zhou Z. Modelling and stability analysis of a high-speed train braking system. International Journal of Mechanical Sciences.

2023; 250(108315): 1–16. http://doi.org/10.1016/j.ijmecsci.2023.108315

31. Kligerman Y., Varenberg M. Elimination of stick-slip motion in sliding of split or rough surface. Tribology Letters. 2014; 53(2): 395–399. http://doi.org/10.1007/s11249-013-0278-8
32. Kröger M., Neubauer M., Popp K. Experimental investigation on the avoidance of self-excited vibrations. Philosophical Transactions of the Royal Society A: Mathematical, Physical and Engineering Sciences. 2008; 366(1866): 785–810. http://doi.org/10.1098/rsta.2007.2127
33. Liu W., Ni H., Wang P., Chen H. Investigation on the tribological performance of micro-dimples textured surface combined with longitudinal or transverse vibration under hydrodynamic lubrication. International Journal of Mechanical Sciences. 2020; 174(105474). https://doi.org/10.1016/j.ijmecsci.2020.105474
34. Zuleeg J. How to measure, prevent, and eliminate stick-slip and noise generation with lubricants. SAE Technical Papers, 2015- June, SAE International; 2015. https://doi.org/10.4271/2015-01-2259
35. Zhu D., Wang J., Wang Q.J. On the stribeck curves for lubricated counterformal contacts of rough surfaces. Journal of Tribology. 2015; 137(2). https://doi.org/10.1115/1.4028881
36. Armstrong-Hélouvry. Control of Machines with Friction. Springer US; 1991. https://doi.org/10.1007/978-1-4615-3972-8
37. Rybkiewicz M., Leus M. Selection of the friction model for numerical analyses of the impact of longitudinal vibration on stick-slip movement. Advances in Science and Technology Research Journal. 2021; 15(3): 277–287. https://doi.org/10.12913/22998624/141184
38. Rybkiewicz M., Gutowski P., Leus M. Experimental and numerical analysis of stick-slip suppression with the use of longitudinal tangential vibration. Journal of Theoretical and Applied Mechanics (Poland). 2020; 58(3): 637–648. https://doi.org/10.12913/22998624/141184
39. Wang P., Ni H., Wang R., Li Z., Wang Y. Experimental investigation of the effect of in-plane vibrations on friction for different materials. Tribology International. 2016; 99: 237–247. https://doi.org/10.1016/j.triboint.2016.03.021
40. Leus M., Gutowski P., Rybkiewicz M. Effectiveness of friction force reduction in sliding motion depending on the frequency of longitudinal tangential vibrations, sliding velocity and normal pressure. Acta Mechanica et Automatica. 2023; 17(4): 490–498. https://doi.org/10.2478/ama-2023-0057
41. Qu H., Zhou N., Guo W., Qu J. A model of friction reduction with in-plane high-frequency vibration. Proceedings of the Institution of Mechanical Engineers, Part J: Journal of Engineering Tribology. 2016; 223(9): 962–967. https://doi.org/10.1177/135065011562101
42. Kapelke S., Seemann W. On the effect of longitudinal vibrations on dry friction: modelling aspects and experimental investigations. Tribology Letters. 2018; 66(3). https://doi.org/10.1007/s11249-018-1031-0
43. Leus M., Gutowski P., Bachtiak-Radka E. The effect of contact compliance of sliding pair on friction force reduction at longitudinal tangential vibrations. Tribology International. 2023; 187. https://doi.org/10.1016/j.triboint.2023.108701
44. Bowden F.P., Tabor D. The Friction and Lubrication of Solids. Oxford: Oxford University Press; 1950.
45. Tolstoi D.M. Significance of the normal degree of freedom and natural normal vibrations in contact friction. Wear. 1967; 10(3): 199–213. https://doi.org/10.1016/0043-1648(67)90004-X
46. Tolstoi D.M., Borisova G.A., Griegorova S.R. Friction reduction by perpendicular oscillation. Doklady Technical Physis. 1973; 17(9): 907–909.
47. Lenkiewicz W. The sliding friction process effect of external vibration. Wear. 1969; 13(2): 99–108. https://doi.org/10.1016/0043-1648(69)90505-5
48. Leus M., Abrahamowicz M. Experimental investigations of elimination the stick-slip phenomenon in the presence of longitudinal tangential vibration. Acta Mechanica et Automatica. 2019; 13(1): 45–50. https://doi.org/10.2478/ama-2019-0007
49. Abdo J., Tahat M., Abouelsoud A. The effect of excitation frequencies on stick-slip amplitude. 3rd International Conference on Integrity, Reliability and Failure, Porto, Portugal: 2009.
50. Abdo J., Tahat M., Abouelsoud A., Danish M. The effect of frequency of vibration and humidity on the stick-slip amplitude. International Journal of Mechanics and Materials in Design. 2010; 6(1): 45–51. https://doi.org/10.1007/s10999-010-9117-3
51. Abdo J., Zaier R. A novel pin-on-disk machine for stick-slip measurements. Materials and Manufacturing Processes. 2012; 27: 751–755.
52. Neubauer M., Neuber C.C., Popp K. Control of stick-slip vibrations. Solid Mechanics and Its Applications. 2005; 130: 223–232.
53. Popp K., Rudolph M. Avoidance of stick-slip motion by vibration control. PAMM Proceedings in Applied Mathematics and Mechanics. 2003; 3(1): 120–121. https://doi.org/10.1002/pamm.200310337
54. Popp K., Rudolph M. Vibration control to avoid stick-slip motion. JVC/Journal of Vibration and Control. 2004; 10(11): 1585–1600. https://doi.org/10.1177/1077546304042026

55. Wang X., Wang R., Huang B., Mo J., Ouyang H. A study of effect of various normal force loading forms on frictional stick-slip vibration. Journal of Dynamics, Monitoring and Diagnostics. 2022; 1(1): 46–55. https://doi.org/10.37965/jdmd.v2i2.48
56. Popov V.L., Starcevic J., Filippov A.E. Influence of ultrasonic in-plane oscillations on static and sliding friction and intrinsic length scale of dry friction processes. Tribology Letters, 2010; 39. https://doi.org/10.1007/s11249-009-9531-6
57. Teidelt E., Starcevic J., Popov V.L. Influence of ultrasonic oscillation on static and sliding friction. Tribology Letters. 2012; 48(1): 51–62. https://doi.org/10.1007/s11249-012-9937-4
58. Luo L., Li N., Li Q., Cheng Z., Wang B., Long W., et al. The inhibition mechanism of ultrasonic vibration on stick-slip phenomenon of sliding friction pair. Scientific Reports. 2024; 14(25847): 1–12. https://doi.org/10.1038/s41598-024-73652-w
59. Luo L., Li Q., Cheng Z., Wang B., Long W., Zhao B. The friction reduction and stick–slip inhibition effects of ultrasonic vibration on sliding friction pair under solid lubrication. Tribology Letters. 2025; 73(1). https://doi.org/10.1007/s11249-025-01969-2
60. Leus M., Rybkiewicz M., Woźniak M. The Influence of normal pressure on the friction force reduction effect caused by longitudinal tangential vibrations. Advances in Science and Technology Research Journal. 2022; 16(6): 14–22. https://doi.org/10.12913/22998624/155055